A Conformational Change in the Catalytic Core of the Hammerhead Ribozyme upon Cleavage of an RNA Substrate†

Jean-Pierre Simorre,‡ Pascale Legault,§ Arlene B. Hangar, Paul Michiels,|| and Arthur Pardi*

Department of Chemistry and Biochemistry, University of Colorado, Boulder, Colorado 80309-0215

Received August 15, 1996; Revised Manuscript Received November 12, 1996⊗

ABSTRACT: Heteronuclear multidimensional NMR structural studies have been performed on a hammerhead ribozyme complexed with a cleaved and an uncleaved substrate. The NMR data demonstrate that the three helices surrounding the conserved catalytic core hammerhead are stably formed in both complexes. Evidence is also presented that indicates that the sheared G-A base pairs in the conserved core are formed in the absence of Mg^{2+}. The NMR structural data demonstrate that there is a significant structural change of the conserved core of the hammerhead ribozyme−substrate complex upon cleavage of the substrate. Molecular dynamics calculations were performed to generate models of the ribozyme-cleaved substrate complex, and these results are used to help understand the mechanism of the hammerhead cleavage reaction.

The hammerhead ribozyme represents the best biochemically, kinetically, and structurally characterized catalytic RNA. The consensus secondary structure and conserved core region for the hammerhead ribozyme were originally proposed by comparing naturally occurring sequences from plant viroids and virusoids (Keese & Symons, 1987). The sequence requirements for the catalytic activity of the hammerhead have been identified by combining the phylogenetic data with *in vitro* studies of mutant hammerhead ribozymes, giving the presently accepted conserved core nucleotides in Figure 1 (Ruffner et al., 1990). In addition to the biochemical and kinetic studies, X-ray crystal structures have been determined for two hammerhead ribozyme−noncleavable substrate complexes (Pley et al., 1994; Scott et al., 1995). The effects of functional group modifications in the conserved core of the hammerhead ribozyme, and how they relate to the three-dimensional structure of the hammerhead, have recently been reviewed (McKay, 1996), but the detailed mechanism by which the hammerhead ribozyme achieves site-specific cleavage of a phosphodiester bond is still not well-understood.

The crystal structures of the hammerhead were solved for ribozyme−noncleavable substrate complexes (Pley et al., 1994; Scott et al., 1995); therefore, at this point there is no direct structural information for the conserved core of a ribozyme-cleaved substrate complex. Nuclear magnetic resonance (NMR)[1] studies have been performed on a cleaved hammerhead (Pease & Wemmer, 1990), showing that the double-helical regions are preserved after cleavage but no information was obtained for the conserved core region. Gel electrophoresis studies show that the mobilities of the cleaved and uncleaved hammerhead complex containing an extended helix I and helix II are very similar in the presence of Mg^{2+} but there are substantial differences for the gel mobility in the absence of Mg^{2+} (Gast et al., 1994). A two-step folding mechanism has been proposed for a noncleavable hammerhead ribozyme−substrate complex where the angle of helix I relative to helices II and III changes as the concentration of Mg^{2+} is increased (Bassi et al., 1995). In addition, transient electric birefringence experiments have been used to measure the angles between the three helices in the hammerhead, and there appears to be little change in the observed angles between the cleaved and uncleaved hammerhead complex in the presence of Mg^{2+} (Amiri & Hagerman, 1994). These techniques only yield information on the global structure of the hammerhead ribozyme but do not give data for structural changes in the conserved core of the hammerhead induced by cleavage of a substrate. In this study, heteronuclear multidimensional NMR experiments are used to probe the structure of the hammerhead ribozyme complexed with cleaved and uncleaved substrates. The NMR data demonstrate that there is a significant structural change in the conserved core of the hammerhead ribozyme upon cleavage. The implications of the observed structural change on the thermodynamics and mechanism for substrate cleavage by the hammerhead ribozyme will be discussed (Hertel et al., 1994; Hertel & Uhlenbeck, 1995).

MATERIALS AND METHODS

All RNAs were prepared by *in vitro* transcription with T7 RNA polymerase using 99% ^{15}N- and/or ^{13}C-labeled

† This work was supported by NIH Grant AI30726 and Research Career Development Award AI01051 to A.P, a NATO/CNRS Fellowship to J.-P.S., and a NSERC 1967 Science and Engineering scholarship and a FCAR scholarship to P.L. We also thank the Colorado RNA Center and the W. M. Keck Foundation for their generous support of RNA research on the Boulder campus.

* Author to whom correspondence should be addressed.

‡ Present address: Institut de Biologie Structurale, CEA-CNRS, 41 Avenue des Martyrs, F-38027 Grenoble Cedex, France.

§ Present address: Department of Molecular and Medical Genetics, One King's College Circle, University of Toronto, Toronto, Ontario, M5S 1A8, Canada.

|| Present address: Department of Biophysical Chemistry, University of Nijmegen, Toernooiveld 1, NL-6525 ED, Nijmegen, The Netherlands.

⊗ Abstract published in *Advance ACS Abstracts,* January 1, 1997.

[1] Abbreviations: HMQC, heteronuclear multiple-quantum correlation; HSQC, heteronuclear single-quantum correlation; NTPs, ribonucleotide triphosphates; NMR, nuclear magnetic resonance; NOE, nuclear Overhauser effect; NOESY, nuclear Overhauser effect spectroscopy; ROESY, rotating frame Overhauser effect spectroscopy; R19, hammerhead ribozyme 19; S19, substrate 19; 2D, two dimensional; 3D, three dimensional.

S0006-2960(96)02052-1 CCC: $14.00

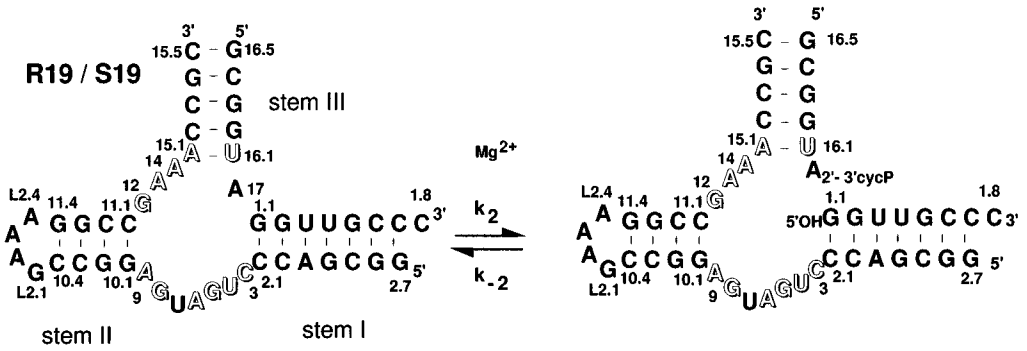

FIGURE 1: Catalytic cleavage reaction for the R19/S19 hammerhead ribozyme. The sequences for the ribozyme and substrate being studied are shown, and the nucleotides in the conserved catalytic core of the hammerhead ribozyme are indicated by outlined characters (Keese & Symons, 1987; Ruffner et al., 1990). The standard numbering system for the hammerhead ribozyme has been employed (Hertel et al., 1992). In the presence of magnesium, the S19 substrate is cleaved at the A17 phosphodiester bond, yielding a 2′,3′-cyclic phosphate for one product and a 5′-hydroxyl for the other product. k_2 and k_{-2} are the kinetic constants for cleavage and ligation, respectively (Hertel et al., 1994).

NTPs as previously described (Milligan et al., 1987; Nikonowicz et al., 1992; Legault, 1995). A 99% uniformly $^{13}C/^{15}N$-labeled ribozyme was titrated with a 99% uniformly ^{15}N-labeled RNA substrate to form a 1:1 complex. A second sample was prepared using an unlabeled ribozyme with an ^{15}N-labeled substrate. The NMR samples were prepared at 1.5 mM in 350 μL (Shigemi Micro cell NMR tube) in 25 mM succinate-d_4, 100 mM NaCl, pH 5.5, and 90% H_2O/10% D_2O. The concentrations of the RNAs were determined by UV absorbance using $\epsilon_{260} = 271 \times 10^3$ and 109×10^3 cm^{-1} M^{-1} for R19 and S19, respectively (Legault, 1995).

2D ^{15}N HSQC, ^{15}N HMQC, and NOESY spectra (Müller, 1979; Kumar et al., 1980; States et al., 1982) were performed on $^{13}C/^{15}N$-R19 alone and the $^{13}C/^{15}N$-R19/^{15}N-S19 complex at 5 and 15 °C. A ^{13}C HSQC spectrum was recorded on this $^{13}C/^{15}N$-R19/^{15}N-S19 complex dissolved in 99% D_2O. To identify the resonances from the substrate, 2D NOESY spectra with and without ^{15}N decoupling during the acquisition time were recorded on the R19/^{15}N-S19 sample. For the cleavage reaction, 50 mM $MgCl_2$ was added directly to the $^{13}C/^{15}N$-R19/^{15}N-S19 sample for a total magnesium concentration of 5 mM. This total $MgCl_2$ concentration was increased to 7 mM 24 h later to accelerate cleavage. ^{31}P and ^1H 1D spectra were performed at 15 and 25 °C for 5 days after adding $MgCl_2$. 2D ^{15}N HSQC and 2D NOESY spectra were recorded on this cleaved sample at 15 °C. The R19/^{15}N-S19 sample was also cleaved by addition of 50 mM $MgCl_2$ to give a total magnesium concentration of 7 mM. The ^1H-decoupled 1D ^{31}P spectra were used to determine the extent of cleavage. A ^{15}N HSQC spectrum and NOESY spectra with and without ^{15}N decoupling were performed on this sample after 5 days of reaction at room temperature.

To suppress the water signal, a 11 echo sequence (Sklenar & Bax, 1987) incorporating pulsed-field gradients was employed in the 1D proton spectra and 2D NOESY spectra, and jump and return pulses were used for the ^{15}N HMQC spectra (Müller, 1979; Plateau & Guéron, 1982). The ^{15}N HSQC pulse sequence incorporated a WATERGATE sequence (Piotto et al., 1992) concatenated with the last reverse INEPT and employed water flip-back (Grzesiek & Bax, 1993).

RESULTS

Resonance Assignment Strategy. Figure 1 shows the sequence of the hammerhead system used in this study, where the ribozyme is termed R19 and the substrate S19. Resonance assignment of the imino protons was obtained using the classical approach based on 2D NOESY experiments where imino protons on neighboring base pairs are connected by an NOE cross-peak (Wüthrich, 1986). The resonance assignment was facilitated by information obtained on complexes that were ^{15}N labeled in both the ribozyme and substrate or only ^{15}N labeled in the substrate. Guanosine and uridine imino protons are readily identified based on the chemical shifts of their bound nitrogens in 2D ^{15}N HMQC or HSQC correlation spectra. The normal imino nitrogen chemical shift range is 140−148 ppm for guanine and 150−160 ppm for uridine (Büchner et al., 1978; Roy et al., 1984). The imino proton resonances on the substrate were identified from NOESY spectra on the unlabeled R19/^{15}N-S19 complex acquired with no ^{15}N decoupling. In these spectra, imino proton resonances on the ^{15}N substrate are split into a doublet by the ~90 Hz $^1J_{^1H^{15}N}$ heteronuclear coupling constant.

Resonance Assignment of the Uncleaved Ribozyme−Substrate Complex. Figure 2 shows the imino proton spectra of the R19 ribozyme before and after titration with the S19 substrate. The peak at 12.1 ppm is from the free ribozyme and was used to follow complex formation. The spectrum and assignment of the R19/S19 complex (Figure 2B) are very similar to those published for a similar hammerhead (Heus & Pardi, 1991a). All imino protons from the three helical stems in the complex are observed and assigned except for the terminal base pair in stem I ($G_{2.7}$), and two terminal base pairs ($U_{16.1}$ and $G_{16.5}$) and a penultimate base pair ($G_{15.4}$) in stem III. The absence of imino proton resonances for terminal base pairs is common in DNA or RNA helices due to kinetic fraying of the ends and rapid exchange of the imino protons with solvent (Pardi et al., 1981). The $G_{2.4}-U_{1.4}$ imino proton resonances are readily assigned to 10.2 and 11.9 ppm, respectively, due to a strong NOE cross-peak between the two imino protons and a NOE cross-peak between $U_{1.4}$ and $U_{1.3}$. The other imino protons in stems I−III were assigned from the NOESY spectra by standard procedures (Wüthrich, 1986). The loop residue $G_{L2.1}$ is involved in a sheared G-A base pair (Heus & Pardi, 1991b; Li et al., 1991), and the imino proton of $G_{L2.1}$ was assigned to 10.5 ppm by comparison with other RNAs containing this GAAA loop (Heus & Pardi, 1991b; Jucker et al., 1996). The resonance assignments for the imino protons in the stems and GAAA loop are given in Figure 2B.

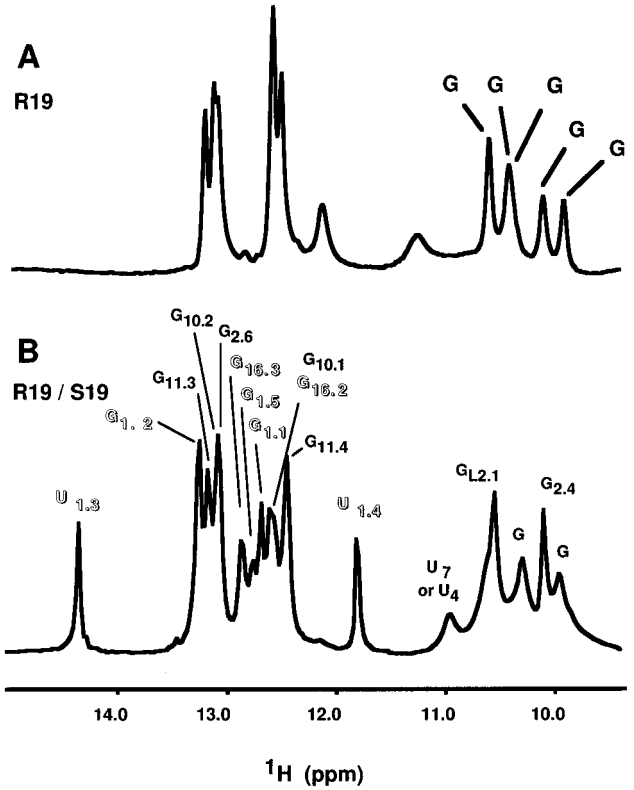

FIGURE 2: Imino proton region of 1D NMR spectra performed on the hammerhead in the absence of Mg^{2+} at 15 °C. The NMR samples were dissolved in 90% H_2O/10% D_2O in buffer containing 25 mM succinate, 100 mM NaCl, pH 5.5. (A) Spectrum of $^{13}C/^{15}N$-R19 before titration with the substrate. The G labels mean that these resonances were identified as G imino protons from the ^{15}N HMQC spectrum performed on the same sample. (B) Imino proton spectrum and assignment of the 1:1 $^{15}N/^{13}C$-R19/^{15}N-S19 complex. The outlined characters indicate that resonances are from the substrate.

The presence of a small amount of free substrate is observed in the ^{15}N HMQC spectrum. These peaks (marked by "f.s." in Figure 5A) are observed in a HMQC spectrum performed on the S19 substrate. A 2D NOESY spectrum performed on this sample does not show any cross-peaks (data not shown); therefore, the cross-peaks in the NOESY spectra of the complex can be unambiguously assigned to molecules in the R19/S19 complex.

At least three of the imino protons resonating below 11.5 ppm in the uncleaved R19/S19 complex could not be assigned to residues in the stems or the GAAA tetraloop (Figure 2B). In the ^{15}N HMQC spectrum of the $^{13}C/^{15}N$-R19/^{15}N-S19 complex, the imino protons at 10.0 and 10.3 ppm give correlation peaks with nitrogens at 144.8 and 145.3 ppm, respectively, and therefore are identified as guanine residues (Büchner et al., 1978; Roy et al., 1984). The peak at 11.0 ppm gives a correlation with a ^{15}N chemical shift in the uridine nitrogen region (158.0 ppm). None of these three resonances are observed in the ^{15}N HMQC performed on the R19/^{15}N S19 complex, demonstrating that they belong to the ribozyme.

Figure 3 shows the $H_{1'}-C_{1'}$ region of a ^{13}C HSQC spectrum on the $^{13}C/^{15}N$-R19/^{15}N-S19 complex in D_2O before addition of $MgCl_2$. The peaks at 3.7 and 4.6 ppm are from two $H_{1'}$ resonances with unusual chemical shifts. The peak at 3.7 ppm was assigned to the $H_{1'}$ of $G_{11.4}$ by comparison with the spectra of other GAAA loops (Heus & Pardi, 1991b; Jucker et al., 1996), and the $H_{1'}$ resonance at 4.6 ppm was tentatively assigned to $G_{10.1}$.

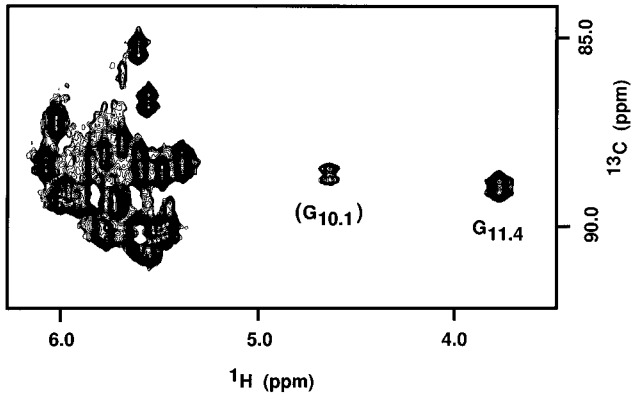

FIGURE 3: $C_{1'}-H_{1'}$ region of the ^{13}C HSQC spectrum of the $^{15}N/^{13}C$-R19/^{15}N-S19 complex performed at 30 °C in D_2O. The two peaks with unusual chemical shifts are assigned to $G_{10.1}$ and $G_{11.4}$ by comparison with other RNAs containing sheared G-A base pairs where the parentheses for $G_{10.1}$ indicate a tentative assignment (see text).

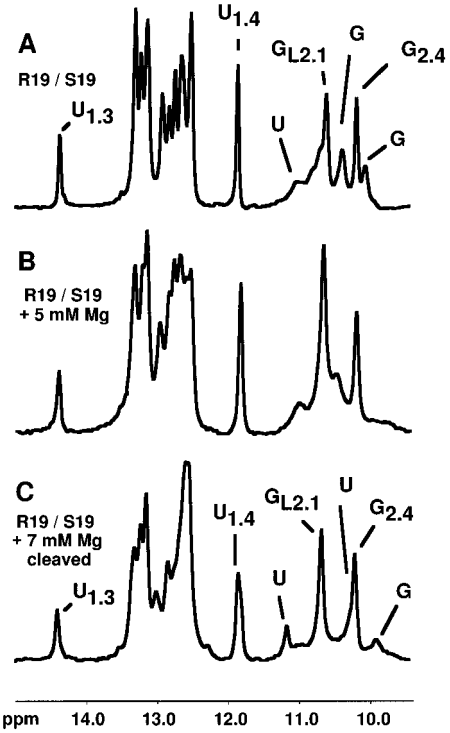

FIGURE 4: Imino proton region of the 1D spectra performed on the 1:1 $^{13}C/^{15}N$-R19/^{15}N-S19 hammerhead complex at 15 °C. (A) R19/S19 complex at pH 5.5 in the absence of Mg^{2+}. (B) Imino proton spectrum for the R19/S19 complex immediately after addition of 5 mM Mg^{2+}. The substrate is not cleaved at this point. (C) Imino proton spectrum of the cleaved R19/S19 complex after five days in the presence of 7 mM Mg^{2+}.

Addition of Magnesium Ions to the Uncleaved Ribozyme−Substrate Complex. 1D ^{31}P and ^1H spectra were performed at various times following addition of Mg^{2+}. Figure 4B shows the spectrum of the $^{13}C/^{15}N$-R19/^{15}N-S19 complex immediately after addition of 5 mM total Mg^{2+}. At this point, the substrate is not cleaved. As discussed under Materials and Methods, after 24 h the Mg^{2+} concentration was increased from 5 to 7 mM total Mg^{2+} to accelerate the cleavage reaction, and this additional Mg^{2+} did not change the 1D proton spectra of the complex. Upon cleavage, the hammerhead ribozyme produces a 2′,3′-cyclic phosphate and

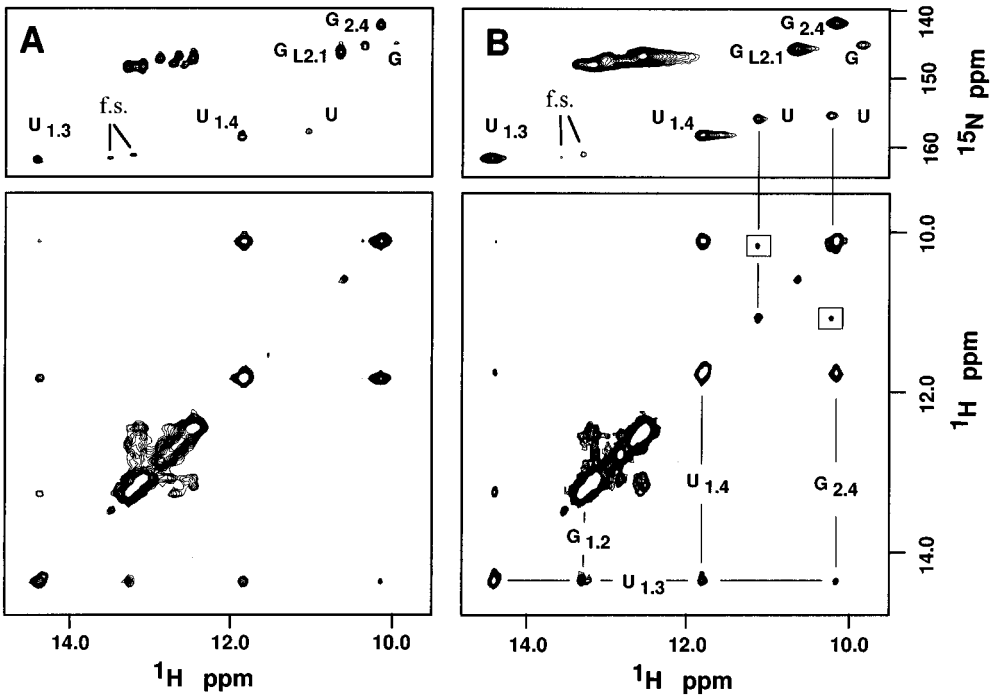

FIGURE 5: Imino region of the 2D ^{15}N HSQC and 2D NOESY spectra performed on the ^{13}C/^{15}N-R19/^{15}N-S19 hammerhead complex. (A) ^{15}N HMQC (top) and 2D NOESY (bottom) spectra performed on the hammerhead at 5 °C before addition of Mg^{2+}. The peaks marked "f.s." correspond to resonances of the free substrate. The total experimental time of the HMQC spectrum was 27 h, with a resolution of 16 Hz in t_1, 4.9 Hz in t_2, 256 transients, and a recovery time of 1.35 s. The NOESY experiment was acquired in 19 h with a resolution of 39 Hz in t_1, 19 Hz in t_2, a mixing time of 200 ms, 112 transients, and a recovery time of 0.9 s. (B) ^{15}N HSQC (top) and 2D NOESY (bottom) experiments performed at 15 °C on the cleaved hammerhead complex in 7 mM added Mg^{2+}. The boxed cross-peaks correspond to a new imino proton to imino proton NOE observed for the cleaved complex. For the ^{15}N HSQC spectrum, the total experimental time was 5 h with a resolution of 46 Hz in t_1, 12 Hz in t_2, 64 transients, and a recovery time of 1 s. The 2D NOESY spectrum was acquired in 24 h with a 39 Hz resolution in t_1, 12 Hz in t_2, 128 transients, and a recovery time of 1 s. The imino proton to imino proton NOEs are illustrated in the NOESY spectrum, and the two U imino protons in the ribozyme that show a strong NOE in the cleaved hammerhead complex are indicated by vertical lines that connect peaks for these protons in the HSQC and NOESY (see text).

a 5′-OH (Symons, 1989). The 2′,3′ cyclic phosphate has a distinct ^{31}P resonance at 21 ppm, and the intensity of this peak was used to monitor of the extent of the cleavage reaction. The intensity of the cyclic phosphate peak in the ^{13}C/^{15}N-R19/^{15}N-S19 sample increased during the first 4 days and then remained constant during the fifth day. Since metal-catalyzed hydrolysis of RNA also yields a 2′,3′-cyclic phosphate, gel electrophoresis was performed on the sample after the NMR experiments, and there was no evidence of degradation of the ribozyme (data not shown).

Resonance Assignment of the Ribozyme−Cleaved Substrate Complex. Figure 4C shows the 1D imino proton spectrum of the hammerhead complex with the cleaved substrate. The NOESY and ^{15}N HSQC spectra on this cleaved complex are shown in Figure 5B. These 2D spectra were performed at 15 °C instead of 5 °C to help reduce possible aggregation. The Watson−Crick base-pairing regions (12−14.5 ppm in ^{1}H) in the spectra of the cleaved and uncleaved complex are not significantly different, except for the larger line widths due to the addition of Mg^{2+}. Analysis of these spectra indicates that the stem base pairs are still formed in the cleaved complex. In the 1D ^{1}H spectrum, the peak at 12.1 ppm is characteristic of the free form of the ribozyme (see Figure 2A), and the weak intensity of this peak in the spectrum of the cleaved complex (Figure 4C) verifies that most of the ribozyme forms a complex with at least one of the cleavage products. The formation of stem I is revealed by the presence of $U_{1.3}$, $U_{1.4}$, and $G_{2.4}$ resonances at the same chemical shifts as before cleavage. An ^{15}N HSQC spectrum on the unlabeled R19/^{15}N-S19 cleaved complex was used to assign the imino protons belonging to the substrate. The ^{15}N HSQC spectra of the cleaved and the uncleaved complex are very similar, although the larger line widths make it difficult to resolve all the resonances. At least four peaks are observed in the guanine imino nitrogen region of the cleaved complex (data not shown). Since there are only three possible base pairs involving substrate G imino protons in stem I, this indicates that stem III is also formed in the cleaved complex.

There are some differences between imino proton spectra of the uncleaved and the cleaved complex in the region below 11.5 ppm (Figures 4 and 5). For the cleaved hammerhead, in addition to the assigned $G_{2.4}$ and $G_{L2.1}$ peaks, there are two U and one G imino peaks in the upfield ^{1}H region of the HSQC spectrum. This region of the ^{15}N HSQC spectrum is quite different in the uncleaved complex where two G and one U imino peaks were observed. The two U imino peaks in the cleaved complex are quite strong, which means that these protons are not exchanging rapidly with solvent. Slow exchange for these two U imino protons is also demonstrated by the presence of these resonances in the 200 ms 2D NOESY spectrum of the cleaved sample. In this experiment, a new cross-peak is observed that connects these two U imino protons at 11.2 and 10.3 ppm (Figure 5B). A 2D ROESY spectrum was acquired on the cleaved complex to test if this cross-peak could arise from a chemical exchange process (Bothner-By et al., 1984; Bax & Davis, 1985). No cross-peak was observed between these two U imino protons in the ROESY spectrum, which indicates no chemical exchange process can be observed between these

two imino proton resonances (data not shown). However the sensitivity in the ROESY experiment is even lower than the NOESY experiment and as seen in Figure 5B, this cross-peak is not very large in the NOESY spectrum; therefore, chemical exchange cannot be completely ruled out. The ratio of the volumes of the diagonal peaks to cross-peaks for these U imino protons did not change between 5 and 15 °C, which suggests that this interaction is not arising from chemical exchange. These U imino proton resonances were assigned to the ribozyme by a ^{15}N HSQC experiment performed on the cleaved hammerhead sample that was only ^{15}N labeled on the substrate. To confirm these assignments, the U imino proton cross-peaks and diagonal peaks were analyzed in NOESY spectra of the R19/^{15}N-S19 complex acquired with and without ^{15}N decoupling. These two U imino protons are unaffected by the ^{15}N decoupling and therefore are unambiguously assigned to the ribozyme.

Model Structures of the Ribozyme−Cleaved Substrate Complex. Restrained molecular dynamics calculations were performed with the program Discover 95.0 (Biosym Inc.) to model the structure of the cleaved hammerhead ribozyme−substrate complex. The modeling started from the X-ray structure of the hammerhead ribozyme−noncleavable substrate complex by McKay and co-workers (Pley et al., 1994). Presently we have only very limited NMR constraints for the cleaved complex so the strategy involved generating a structure as close as possible to the X-ray structure while still being consistent with the NMR data. Molecular dynamics calculations were performed where all residues except 1.1, 2.1, 3−8, and 17 (Figure 1) were fixed during the calculation. Since the NMR results demonstrate that the imino protons of U_4 and U_7 are close in space in the cleaved complex, these two imino protons were constrained to be within 4.5 Å in the molecular dynamics calculations. Two different calculations were performed: one that used the dC at the cleavage site and a second where the dC in the X-ray structure was changed to dA. The calculations used the standard Discover default parameters except that no electrostatics were included. Starting from the coordinates of the X-ray structure and including the U_4-U_7 distance constraint, 2 ps of restrained dynamics was performed at 200 K followed by 1 ps of dynamics at 100 K. The scaling term for the van der Waals interactions started at 0.72 and was increased to 1 during the first 2 ps of dynamics. After the dynamics, 100 steps of conjugate gradient minimization were performed where only residues 1.1, 2.1, 3−8, and 17 were allowed to move, and finally 300 steps of conjugate gradient minimization were performed where all atoms in the molecule were allowed to move.

DISCUSSION

Local Structure of the Hammerhead in the Absence of Magnesium Ion. Resonance assignment of the R19/S19 spectrum in Figure 2B shows that the three stems are formed in the absence of magnesium ion. Imino proton resonances are not observed for the G-C base pairs at the 5′-3′ termini of stems I and III. The rate of exchange of an imino proton with water is generally much faster for a base pair next to the 5′-3′ end of the helix than for a base pair that is next to an internal or hairpin loop. Imino proton resonances are observed for the $G_{1.1}$-$C_{2.1}$ and $G_{10.1}$-$C_{11.1}$ base pairs on stems I and II that are adjacent to the conserved catalytic core of the hammerhead, and the chemical shifts for these base pairs are consistent with standard Watson−Crick base pairs (Wijmenga et al., 1993). However, no imino proton resonance was observed for $U_{16.1}$, indicating that this proton is in fast exchange with solvent. In the X-ray structures of the hammerhead (Pley et al., 1994; Scott et al., 1995), residue 16.1 is involved in a non-Watson−Crick base pair that has only a single hydrogen bond between the amino group of $A_{15.1}$ and the O_4 oxygen of $T_{16.1}/U_{16.1}$. Thus, the absence of the $U_{16.1}$ imino proton resonance in the spectrum in Figure 2B means that this proton is exchanging rapidly with water, which is consistent with the $A_{15.1}$-$dT_{16.1}/A_{15.1}$-$U_{16.1}$ non-Watson−Crick base pair observed in the X-ray structures of the hammerhead (Pley et al., 1994; Scott et al., 1995).

At least three imino protons resonating between 9.5 and 11.5 ppm could not be specifically assigned in the hammerhead complex (Figures 2B and 5A). The peak at 11.0 ppm is from U_7 or U_4 in the core of the hammerhead (see Results). For the two G imino protons at 10.0 and 10.3 ppm, similar upfield-shifted ^{1}H resonances have been observed for sheared G-A base pairs in DNA and RNA duplexes (Heus & Pardi, 1991b; Li et al., 1991; Chou et al., 1992), so these two imino protons are tentatively assigned to G_8 and G_{12} which form part of domain II in the hammerhead core (Pley et al., 1994).

The formation of these sheared G-A base pairs in solution is also supported by the unusual $H_{1'}$ chemical shifts in the ^{13}C HSQC (Figure 3). In some sheared G-A base pairs, such as $G_{L2.1}$-$A_{L2.4}$ in the GAAA tetraloop, the base of $A_{L2.4}$ is positioned over the $H_{1'}$ of the following residue which leads to a large upfield shift of this proton due to the ring current of the adenosine (Heus & Pardi, 1991b; Jucker et al., 1996). Based on the X-ray structures, a large upfield shift is also predicted for the $H_{1'}$ of $G_{10.1}$, but no upfield shift is expected for the $H_{1'}$ of A_{14} which is next to the sheared G_8-A_{13} base pair (Pley et al., 1994; Scott et al., 1995). As seen in Figure 3, two $H_{1'}$ resonances are shifted upfield, and, as discussed above, the resonance at 3.7 ppm is assigned to the $H_{1'}$ of $G_{11.4}$. The second shifted $H_{1'}$ is tentatively assigned to $G_{10.1}$, and is consistent with formation of the sheared G_{12}-A_9 base pair that is observed in the X-ray structures of the hammerhead ribozyme (Pley et al., 1994; Scott et al., 1995).

Addition of Mg^{2+} to the Hammerhead Ribozyme−Substrate Complex. The cleavage reaction was initiated by addition of $MgCl_2$ directly in the NMR tube. As previously observed for a DNA substrate (Heus & Pardi, 1991a), the imino proton region of the uncleaved hammerhead spectrum is not significantly altered by the addition of Mg^{2+} (Figure 4A,B). The extent of the cleavage reaction was readily followed by monitoring the intensity of the peak for the 2′,3′-cyclic phosphate at 21 ppm in the 1D ^{31}P spectra. Analysis of the ^{31}P spectra gave a half-life for cleavage of the S19 substrate by the R19 ribozyme of ∼2 days ($k_2 \sim 10^{-4}$ min^{-1}). The k_2 for substrate cleavage of other hammerheads has been measured under different conditions (Dahm et al., 1993; Hertel & Uhlenbeck, 1995), but correcting for the temperature, the pH, and the estimated Mg^{2+} concentration, the half-life for cleavage under the NMR conditions is predicted to be 6−10 h ($k_2 \sim 10^{-3}$ min^{-1}). This difference between the predicted and measured half-lives could result from errors in estimating the free Mg^{2+} concentration and/or from aggregation effects at the high NMR concentrations. It is impossible to determine accurately the free Mg^{2+} concentration of a solution containing ∼1 mM RNA by simply adding

a known amount of Mg^{2+} because of the large number of metal ion binding sites in the RNA; therefore, only the total Mg^{2+} concentration is reported.

Local Structure of the Stems in the Hammerhead after Cleavage of the Substrate. 1D and 2D spectra of the ribozyme-cleaved substrate complex are shown in Figures 4C and 5B and can be compared to the spectra of the uncleaved complex in Figures 4A, 4B, and 5A. As discussed above, for the uncleaved complex, the imino proton spectrum can be used to confirm formation of the complex after cleavage (Figure 4C). The weak intensity of the peak at 12.2 ppm (Figure 4C), which is characteristic of the free hammerhead (Figure 3A), indicates that the concentration of the free hammerhead is very low after cleavage of the substrate. Imino proton−imino proton NOESY cross-peaks are observed for $G_{1.1}$ to $G_{1.2}$, $G_{1.2}$ to $U_{1.3}$, $U_{1.3}$ to $U_{1.4}$, and $U_{1.4}$ to $G_{2.4}$. Slow exchange observed for these imino protons demonstrates that the region next to the cleavage site is not highly dynamic even when the substrate is cleaved. The number and type of slowly exchanging imino protons belonging to the substrate were determined from the 2D ^{15}N HSQC experiment on the cleaved R19/^{15}N S19 sample. In the G-C base-paired region of this spectrum (11.5−14 ppm for ^{1}H and 140−152 ppm for ^{15}N), at least four guanine imino protons are observed. Since stem I has only three G residues in the substrate, at least one G imino proton arises from a G-C base pair in stem III in the cleaved substrate.

These results demonstrate that stems I and III are still formed after cleavage of the substrate. The similar chemical shifts of the imino protons in the stems before and after cleavage, and the similar pattern of NOESY cross-peaks for these imino protons, indicate that the structures of the three stems are not greatly altered by cleavage. Absence of significant conformational changes in the stems upon cleavage has been observed for two other hammerheads (Pease & Wemmer, 1990; Gast et al., 1994).

A Conformational Change in the Conserved Core of the Hammerhead after Cleavage of the Substrate. An important difference between the NOESY spectra of the cleaved and uncleaved complexes is that a new cross-peak is observed between two U imino protons in the cleaved complex (Figure 5B). This cross-peak has similar intensity to NOEs for imino protons on neighboring base pairs in the stems of the hammerhead. In addition, the ratio of these U_4 and U_7 imino proton cross-peaks to their diagonal peaks indicates that these protons are much closer together than imino protons on neighboring base pairs, consistent with a U-U base pair. In a U-U base pair, the distance between the two imino protons is very short, leading to a very strong NOE. The chemical shifts of these two imino protons are also consistent with a hydrogen bond with an oxygen. NMR spectra have been obtained on other RNAs duplexes containing U-U base pairs (Santa Lucia et al., 1991; Nikonowicz & Pardi, 1992, 1993), and the chemical shifts for those U-U base pairs are almost identical to those observed here.

Thus, the NMR data in Figure 5 are consistent with two U imino protons observed in the cleaved hammerhead being involved in a U-U base pairing, whereas there is no NMR evidence for such an interaction in the uncleaved complex. The ^{15}N HSQC spectrum and NOESY spectra with or without ^{15}N decoupling for this cleaved R19/^{15}N-S19 complex unambiguously demonstrated that both of the U imino protons belong to the ribozyme and are assigned to U_4 and U_7. In the X-ray structure, U_7 is stacked above $T/U_{16.1}$, and U_4 is in the U-turn where its imino proton forms a hydrogen bond with a phosphate (see Figure 6A) (Pley et al., 1994; Scott et al., 1995). The distance between the U_4 and U_7 imino protons in the X-ray structure of the uncleaved complex is ≈10 Å whereas from the NOESY spectra it is estimated that these two protons are close in the cleaved hammerhead complex. This means that there is a substantial difference between the solution structure of the cleaved hammerhead complex and the crystal structure of the uncleaved complex.

Starting from the X-ray structure by McKay and coworkers (Pley et al., 1994), we generated 3D models consistent with the NMR data where very local changes in the core lead to conformations that have the U_4 and U_7 imino protons close together. Molecular dynamics calculations were performed where the structure of the ribozyme−substrate complex was kept as close as possible to the X-ray structure while still allowing for conformational changes that bring together the U_4 and U_7 imino protons (see Results). Two model structures consistent with the NMR data are shown in Figure 6B,C. In both these models, the stacking of U_7 with $T_{16.1}$ is disrupted, and the U-turn motif in the ribozyme is modified by breaking the U_4 imino proton to phosphate hydrogen bond. In comparing the X-ray structure (Figure 6A) with the model calculations (Figure 6B,C), the nucleotide that undergoes the largest conformational change is U_7, where this residue turns around to face the U-turn and interact with U_4. Note that very similar models for the cleaved substrate can be generated whether there is a dC and dA at the cleavage site (Figure 6B,C). Because we do not have structure constraints involving the cleaved substrate, these model structures were generated on the uncleaved substrate. Thus, in the true ribozyme−cleaved substrate complex, one might expect there would be even larger conformational changes than those seen in Figure 6B,C, since cleaving of the substrate would introduce additional degrees of freedom. Although Figure 6B and Figure 6C are only models of the ribozyme bound to the cleaved substrate, it is interesting to note that G_5 is brought closer to the cleavage site. G_5 is one of the anomalies in trying to understand the structure−function of the hammerhead ribozyme since a large number of G_5 modifications inhibit activity (McKay, 1996) yet in the X-ray structures of the ribozyme−noncleavable substrate complex this residue is not involved in significant intramolecular interactions (Pley et al., 1994; Scott et al., 1995). Thus, structural information on the hammerhead ribozyme−product complex could represent an alternate model of the catalytically active species and might aid in understanding the function for G_5. However, it is important to realize that it is not possible to generate a unique and reliable model of the conserved core in the cleaved hammerhead complex given our limited NMR data, and Figure 6B,C shows only two of a range of conformations that are consistent with the observed data.

Kinetic and Thermodynamic Implications of the Conformational Change in the Core of the Cleaved Hammerhead. Thermodynamic parameters have been determined for the cleavage reaction catalyzed by the hammerhead ribozyme (Hertel et al., 1994; Hertel & Uhlenbeck, 1995). The equilibrium constant for the reaction in Figure 1 was determined to be ≈70 at 15 °C by measuring the rate constants for the ligation and cleavage reactions (using a

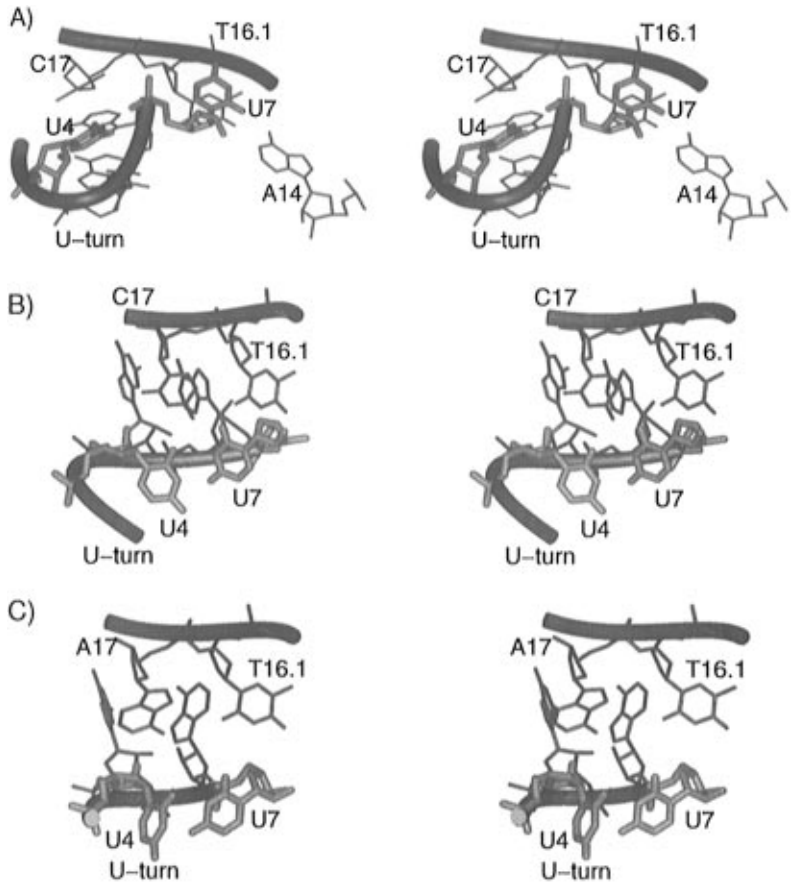

FIGURE 6: (A) Stereoview of part of the catalytic core of the X-ray structure of the hammerhead ribozyme−noncleavable substrate complex (Pley et al., 1994). Nucleotides U_4-U_7, A_{14}, $T_{16.1}$, and C_{17} are shown, and the ribbons correspond to the sugar−phosphate backbone. In the X-ray structure, U_7 forms a single hydrogen bond with A_{14}, and the U_7 and U_4 imino protons are far apart. (B) Stereoview of a model of the catalytic core region generated by molecular dynamics calculations where the imino protons of U_4 and U_7 are restrained to be close together (<4.5 Å). The same residues are shown as in (A) except that residue A_{14} is not shown. This model was generated from the X-ray structure where only residues 1.1, 2.1, 3−8, and 17 were allowed to move in the calculation (see text). (C) Stereoview of a second molecular dynamics-generated model of the catalytic core region that started from the X-ray structure except that dC_{17} was changed to dA to better mimic the complex employed in the NMR studies (see text).

slightly different hammerhead system) (Hertel et al., 1994; Hertel & Uhlenbeck, 1995). This cleavage reaction is not enthalpically driven ($\Delta H \approx 10$ kcal/mol) but instead results from a gain in entropy ($\Delta S \approx 44$ eu). As proposed by Uhlenbeck and co-workers, possible reasons for this entropy change are an increase in the degrees of freedom of the ribozyme−product complex, or a difference in solvation or metal binding upon cleavage (Hertel et al., 1994). The NMR data here demonstrate that the imino protons of U_4 and U_7 are close together in the cleaved hammerhead ribozyme−substrate complex, and are consistent with formation of a U-U base pair. These imino protons also exchange more slowly with solvent in the cleaved hammerhead complex than they do in the uncleaved complex. Thermodynamic studies have shown that U-U base pairs stabilize helix formation in model RNA duplexes (Santa Lucia et al., 1991) and thus formation of a U-U base pair could stabilize the cleaved hammerhead ribozyme−substrate complex.

It is somewhat surprising that U_7 is involved in the conformational change in the conserved core because it is the only nonconserved residue in the catalytic core of the hammerhead, and the hammerhead ribozyme is active with G, A, or C at this position (Ruffner et al., 1990). However, recent studies show that the k_2 for hammerhead catalysis varies by over 100-fold for base substitutions at residue 7 (Burgin et al., 1996). A 10-fold increase in k_2 was found for a pyridin-4-one substitution at residue 6 whereas k_2 decreased by ~15-fold for a 6-aza-U substitution. Thus, it does not appear that residue 7 is a completely inactive player in the catalytic reaction as was hypothesized from the kinetic data on the natural mutants. In the X-ray structure of the hammerhead, U_7 forms a hydrogen bond with A_{14} (see Figure 6A), but this hydrogen bond would be disrupted in most of the other base substitutions at residue 7; thus, at present there is no obvious correlation with functional group substitutions at this site and catalytic activity (Burgin et al., 1996).

If U_7 forms a U-U base pair with U_4 in the cleaved complex, then changing U_7 to an A, C, or G would disrupt or modify the base pair and affect the stability of the ribozyme−product complex. Although k_2 has been determined for base modifications at position 7 (Keese & Symons, 1987; Ruffner et al., 1990), there is no information on the rate of ligation, k_{-2} (or on the equilibrium constant between the uncleaved and the cleaved complex), for different nucleotides at position 7. If U_7 is involved in a stabilizing interaction in the cleaved complex, then disrupting this interaction should increase the rate of ligation and therefore shift the internal equilibrium toward ligation instead of cleavage. In another small ribozyme system, the hairpin ribozyme, the internal equilibrium is close to 1 (Buzayan et al., 1986), and therefore one sees equal concentrations of the cleaved and ligated products at equilibrium. A confor-

mational change leading to stabilizing interactions in the cleaved hammerhead ribozyme−substrate complex could help explain the observed thermodynamic equilibrium for the hammerhead ribozyme which favors cleavage over ligation by over a factor of 70. Since a U at position 7 is not required for catalytic activity of the hammerhead ribozyme (Ruffner et al., 1990), it would be interesting to measure the internal equilibrium for hammerhead ribozymes with different nucleotides at U_7 to see if the internal equilibrium is shifted more toward ligation.

CONCLUSIONS

As recently reviewed by McKay (1996), the two X-ray structures of the hammerhead ribozyme do not explain all the kinetic data with mutant and modified nucleotides, and it is clear that there must be a conformational change from the crystal structures to obtain a catalytically active conformation. At this point, it is not known how closely the conformation of the "ground state" crystal structures of the hammerhead ribozyme−noncleavable substrate complexes mimics the transition state, and it would be useful to have structural data on transition state analogues or other reaction intermediates of the hammerhead (McKay, 1996). Unfortunately, good transition state analogues of the hammerhead cleavage reaction are not yet available, and therefore one must pursue other structural mimics of the catalytically active structures. It is possible that the ribozyme−product complex represents as good a model for the catalytically active species as the ribozyme−substrate complex. The heteronuclear NMR experiments performed here show that there is a substantial structural change in the U-turn region of the cleaved hammerhead ribozyme−substrate complex, and the NMR results are consistent with a structure that brings G_5 close to the cleavage site. The present NMR data are too limited to generate a detailed structure, and we are presently pursuing complete resonance assignment of the hammerhead ribozyme to generate better structural information. It would be interesting to have both NMR and X-ray structures of the ribozyme−product complex, because this structure may represent a useful model for probing the enzymatic mechanism of the hammerhead ribozyme.

ACKNOWLEDGMENT

We thank Dr. O. C. Uhlenbeck for a critical reading of the manuscript and Drs. Uhlenbeck and B. Clouet-d'Orval for very useful discussions.

REFERENCES

Amiri, K. M. A., & Hagerman, P. J. (1994) *Biochemistry 33*, 13172−13177.
Bassi, G. S., Mollegaard, N. E., Murchie, A. I. H., Vonkitzing, E., & Lilley, D. M. J. (1995) *Nat. Struct. Biol. 2*, 45−55.
Bax, A., & Davis, D. G. (1985) *J. Magn. Reson. 63*, 207−213.
Bothner-By, A. A., Stephens, R. L., Lee, J. M., Warren, C. D., & Jeanloz, R. W. (1984) *J. Am. Chem. Soc. 106*, 811−813.
Büchner, P., Maurer, W., & Rüterjans, H. (1978) *J. Magn. Reson. 29*, 45−63.
Burgin, A. B., Jr., Gonzalez, C., Matulic-Adamic, J., Karpeisky, A. M., Usman, N., McSwiggen, J. A., & Beigelman, L. (1996) *Biochemistry 35*, 14090−14097.
Buzayan, J. M., Gerlach, W. L., & Bruening, G. (1986) *Nature 323*, 349−353.
Chou, S. H., Cheng, J. W., & Reid, B. R. (1992) *J. Mol. Biol. 228*, 138−155.
Dahm, S. C., Derrick, W. B., & Uhlenbeck, O. C. (1993) *Biochemistry 32*, 13040−13045.
Gast, F. U., Amiri, K. M. A., & Hagerman, P. J. (1994) *Biochemistry 33*, 1788−1796.
Grzesiek, S., & Bax, A. (1993) *J. Am. Chem. Soc. 115*, 12593−12594.
Hertel, K. J., & Uhlenbeck, O. C. (1995) *Biochemistry 34*, 1744−1749.
Hertel, K. J., Pardi, A., Uhlenbeck, O. C., Koizumi, M., Ohtsuka, E., Uesugi, S., Cedergren, R., Eckstein, F., Gerlach, W. L., Hodgson, R., & Symons, R. H. (1992) *Nucleic Acids Res. 20*, 3252.
Hertel, K. J., Herschlag, D., & Uhlenbeck, O. C. (1994) *Biochemistry 33*, 3374−3385.
Heus, H. A., & Pardi, A. (1991a) *J. Mol. Biol. 217*, 113−124.
Heus, H. A., & Pardi, A. (1991b) *Science 253*, 191−194.
Jucker, F. M., Heus, H. A., Yip, P. F., Moors, E. H. M., & Pardi, A. (1996) *J. Mol. Biol. 264*, 968−980.
Keese, P., & Symons, R. H. (1987) in *Viroids and Viroid-like Pathogens* (Semancik, J. S., Ed.) pp 1−47, CRC Press, Boca Raton.
Kumar, A., Ernst, R. R., & Wüthrich, K. (1980) *Biochem. Biophys. Res. Commun. 95*, 1−6.
Legault, P. (1995) Ph.D. Thesis, University of Colorado, Boulder.
Li, Y., Zon, G., & Wilson, W. D. (1991) *Proc. Natl. Acad. Sci. U.S.A. 88*, 26−30.
McKay, D. B. (1996) *RNA 2*, 395−403.
Milligan, J. F., Groebe, D. R., Witherell, G. W., & Uhlenbeck, O. C. (1987) *Nucleic Acids Res. 15*, 8783−8789.
Müller, L. (1979) *J. Am. Chem. Soc. 101*, 4481−4484.
Nikonowicz, E. P., & Pardi, A. (1992) *Nature 355*, 184−186.
Nikonowicz, E. P., & Pardi, A. (1993) *J. Mol. Biol. 232*, 1141−1156.
Nikonowicz, E. P., Sirr, A., Legault, P., Jucker, F. M., Baer, L. M., & Pardi, A. (1992) *Nucleic Acids Res. 20*, 4507−4513.
Pardi, A., Martin, F. H., & Tinoco, I., Jr. (1981) *Biochemistry 20*, 3986−3996.
Pease, A. C., & Wemmer, D. E. (1990) *Biochemistry 29*, 9039−9046.
Piotto, M., Saudek, V., & Sklenar, V. (1992) *J. Biomol. NMR 2*, 661−665.
Plateau, P., & Guéron, M. (1982) *J. Am. Chem. Soc. 104*, 7310−7311.
Pley, H. W., Flaherty, K. M., & McKay, D. B. (1994) *Nature 372*, 68−74.
Roy, S., Papastavros, M. Z., Sanchez, V., & Redfield, A. G. (1984) *Biochemistry 23*, 4395−4400.
Ruffner, D. E., Stormo, G. D., & Uhlenbeck, O. C. (1990) *Biochemistry 29*, 10695−10702.
Santa Lucia, J., Kierzek, R., & Turner, D. H. (1991) *Biochemistry 30*, 8242−8251.
Scott, W. G., Finch, J. T., & Klug, A. (1995) *Cell 81*, 991−1002.
Sklenar, V., & Bax, A. (1987) *J. Magn. Reson. 74*, 469−479.
States, D. J., Haberkorn, R. A., & Ruben, D. J. (1982) *J. Magn. Reson. 48*, 286−292.
Symons, R. H. (1989) *Trends Biochem. Sci. 14*, 445−450.
Wijmenga, S. S., Mooren, M. M. W., & Hilbers, C. W. (1993) in *NMR of Macromolecules* (Roberts, G. C. K., Ed.) pp 217−288, Oxford University Press, Oxford.
Wüthrich, K. (1986) *NMR of Proteins and Nucleic Acids*, John Wiley & Sons, New York.

BI9620520